

Room Temperature Self-Healing in Soft Pneumatic Robotics

Terryn, Seppe; Roels, Ellen; Brancart, Joost; Van Assche, Guy; Vanderborght, Bram

Published in:
IEEE Robotics & Automation Magazine

DOI:
[10.1109/MRA.2020.3024275](https://doi.org/10.1109/MRA.2020.3024275)

Publication date:
2020

Document Version:
Accepted author manuscript

[Link to publication](#)

Citation for published version (APA):

Terryn, S., Roels, E., Brancart, J., Van Assche, G., & Vanderborght, B. (2020). Room Temperature Self-Healing in Soft Pneumatic Robotics: Autonomous Self-Healing in a Diels-Alder Polymer Network. *IEEE Robotics & Automation Magazine*, 27(4), 44-55. [9288989]. <https://doi.org/10.1109/MRA.2020.3024275>

Copyright

No part of this publication may be reproduced or transmitted in any form, without the prior written permission of the author(s) or other rights holders to whom publication rights have been transferred, unless permitted by a license attached to the publication (a Creative Commons license or other), or unless exceptions to copyright law apply.

Take down policy

If you believe that this document infringes your copyright or other rights, please contact openaccess@vub.be, with details of the nature of the infringement. We will investigate the claim and if justified, we will take the appropriate steps.

Room-temperature self-healing in soft pneumatic robotics

Sepe Terry^{1,2*}, Joost Brancart², Ellen Roels^{1,2}, Guy Van Assche² and Bram Vanderborght¹.

Healable soft robotic systems have been developed by constructing their flexible membranes out of Diels-Alder polymer networks. In these components, relatively large damages in the centimetre scale can be healed, provided that the temperature is increased to 80-90 °C. This paper presents a new Diels-Alder polymer network that can heal at room temperature by smart design of the network, increasing the molecular mobility in the material at room temperature. This new material is used to develop the first healable soft robotic prototype that can recover its performance from large, realistic damages entirely autonomously. The soft pneumatic hand can heal various damages, including being cut completely in half, without the need for a temperature increase. After healing, the performance of the soft robotic prototype is recovered.

Introduction

Soft robots can resist high mechanical impacts [1][2]. However, throughout their lifetime they are susceptible other damaging conditions. They are prone to fatigue, which is the formation of microscopic cracks that propagate into macroscopic defects. In addition, their membranes can be perforated or cut by a sharp object, such as broken glass, a sharp corner, a nail or a splinter. Soft grippers [3][4] are being designed to manipulate delicate fruits and vegetables in agriculture and food packaging. Sharp twigs, thorns, plastic or glass can end up on the sorting lines and can damage these grippers. Damage can influence the performance of the soft component. If the membrane of a pneumatic soft actuator is perforated, fluid escapes, and the actuator performance decreases. In many cases the actuator can be used in this low efficient, damaged state for a limited time span, as the cut or perforation will tear further, leading to complete failure.

Many soft actuators are constructed out of silicone-based elastomeric networks, such as the *Ecoflex*TM series of *Smooth-On* [5][6]. These elastomers are not expensive, and therefore it is relatively cheap to produce soft actuators. One way to solve the problem of a failed soft actuator is by replacing it completely with a new one. Although being cheap in production, the replacement of a soft actuator can be costly, since it is usually done through human intervention. Most soft actuators are manufactured through casting silicone monomers in a (3D printed) mould, followed by a curing step. During curing, the silicone based network is formed by irreversibly crosslinking. The permanently formed crosslinks do not allow the material to be reprocessed. Consequently, like most elastomeric polymers, these silicone-based networks are not recyclable. Hence, replacing failed soft actuators by new cheaply produced parts is not the most ecological solution. Alternatively, the vulnerability of soft robots can be addressed by over-dimensioning the robotic components with large safety factors, avoiding the possibility of damage in dangerous situations. However, this leads to

larger designs and less energy efficient systems, while potentially compromising the soft and safe characteristic.

Recently, by using smart materials, soft robotic designs are being improved and new actuation principles are generated [7]. This includes the use of shape memory, piezoelectric and self-healing materials, integrating embodied intelligence [8]. In previous work [9]–[12], soft robotic actuators were developed out of self-healing (SH) polymers, more specifically out of reversible elastomeric networks. The crosslinks in these elastomers are reversible Diels-Alder (DA) bonds and provide the material with a healing ability [13]. Macroscopic damages, like perforations and cuts, as well as microscopic fatigue cracks can be healed by heating these flexible materials. Out of these, SH soft grippers and SH soft hands were constructed [9][14]. All could recover entirely from realistic damages. Incorporating a healing function is a eco-friendlier solution to the vulnerability of soft robotics. In addition, a healing ability allows reducing the over-dimensioning of systems, optimizing the design based on the function to perform, instead of based on potential damaging conditions. If these healable actuators are damaged very badly, they can still be recycled, because the reversible characteristic of the crosslinks in the network allows reprocessing [9]. This can further decrease their ecological footprint. For successful healing, typically a temperature increase to 80 °C is required. This can be done by heating the entire soft robotic part (the soft gripper [9]) in a healing station (e.g. an oven) or by integrating a heating device in the actuator design [15]. The need for a heat stimulus provides a certain control over the healing process. However, additional controlled heating systems are required, making the overall robotic system larger and more complex.

This research focusses on lowering the healing temperature of DA polymers towards room temperature, avoiding the need of an additional heating system. Such polymers that do not need an external stimulus to heal, other than the mechanical force of the formation of the damage itself, are called autonomous SH polymers. This paper first introduces different mechanisms for autonomous healing that hold potential for soft robotics. Next, it gives a detailed explanation on how an autonomous SH DA polymer was synthesized. Healing at 25 °C is validated experimentally through extensive tensile testing. The applicability of this DA network for soft robotics is proven through the development of a soft hand prototype that is able to heal autonomously from damage in the centimetre scale. Lastly, we address the recovery of the component's properties after healing.

Autonomous self-healing polymers

There exist in literature many autonomous SH polymers, relying on divergent healing mechanisms. *Extrinsic* autonomous SH polymers rely on healing agents that are embedded in micro/nano-capsules [16]. These extrinsic mechanisms have the downside that the healing action can only take place a limited number of times at the same damage location. In addition, the healing mechanism usually only allows healing relatively small damages. For the capsules to crack open, their shell has to have a brittle characteristic and the matrix material has to be stiffer than the shell material

1) Robotics and Multibody Mechanics (R&MM), Vrije Universiteit Brussel (VUB) and Flanders Make, Pleinlaan 2, B-1050 Brussels, Belgium. <http://mech.vub.ac.be/robotics>.

*e-mail: seterry@vub.be

2) Physical Chemistry and Polymer Science (FYSC), Vrije Universiteit Brussel (VUB), Pleinlaan 2, B-1050 Brussels, Belgium. <http://www.vub.ac.be/MACH/FYSC/>.

[16]. Consequently, extrinsic healing mechanisms work well for thermoset matrices, but they are not adequate for elastomers. Although having potential for hard polymer components in robotics, extrinsic SH polymers are not interesting to construct flexible soft robotic components.

There exist *intrinsic* autonomous SH polymers that have a healing mechanism that works at room temperature. These rely on reversible bonds or complexes with fast dynamics at room temperature. A particularly impressive example is the hydrogel presented by Leibler et al. [17], a supramolecular network formed through physical hydrogen bonds. When slicing these materials, the hydrogen bonds are locally mechanically broken, producing many non-associated groups near the fracture surface that are “eager” to link again. When pressing the fracture surfaces back together immediately after damage, these non-associated groups will reform hydrogen bonds and the cut can be healed at room temperature. Using tensile tests, Leibler proved that after three hours of mending, up to 90% of the original strength was regained.

More recently the SupraPolix Company has reported on another autonomous SH elastomer, “SupraB” [18], with high potential for soft robotics. This supramolecular material is formed by hydrogen bond complexes that act as physical crosslinks. Again when cut, the hydrogen complexes are de-bonded and free groups are created at the fracture surface, which can reconnect when the fracture surfaces are pressed back together. Using hydrogen bond complexes as crosslinks not only enhances the strength of polymer, it also allows faster healing. This is explained by the fact that a firm physical crosslink can already be established when only a fraction of the hydrogen bonds of the complex have been formed. This is the case for SupraB, for which a part of its strength is recovered instantaneously after placing the fracture surfaces together [18][19]. Longer healing times increase the strength further, since an increasing fraction of hydrogen bonds is formed in the crosslink complex.

It is important to mention that aside from the DA polymer used in this work, other autonomous intrinsic SH polymers, relying on various mechanisms, have suitable mechanical and healing properties to introduce healability with high efficiency in soft robotics. Other intrinsic SH polymers with interesting properties (Young’s modulus E , fracture stress σ , fracture strain ϵ and healing efficiency η at 25 °C) are listed in Table 1 and others in a review paper [20].

Table 1: Autonomous SH networks suitable for soft robotics.

Reversible reaction	Institution	E (MPa)	σ (max) (MPa)	ϵ (max) (%)	η at 25 °C (%)
Hydrogen	SupraPolix [18]	0.8	0.350	250	90 (24h)
	ESPCI [17]	0.25	3.0	550	90 (3h)
	UC [21]	17	1.94	780	90 (24h)
Metal-ligand	SU [22]	0.5	0.25	4500	90 (48h)
Exchange	Cidtec [23]	0.05	0.5	3000	97 (24h)
Diels-Alder	VUB	0.12	0.1	245	80-97 (7-14d)

Healing in Diels-Alder networks

DA polymers are networks containing reversible covalent crosslinks, formed by a DA bond between a furan and a maleimide (Fig. 1A). The networks are formed using two monomers; a furan-functionalized Jeffamine (FTx) and a bismaleimide (DPBM) (details in section Reagents). The DA reaction between a furan and a maleimide is an equilibrium reaction and consequently the crosslink bonds are dynamic. This means that for a specific temperature (in equilibrium conditions), a crosslink density can be defined. Although the crosslink density remains constant if the temperature remains

unchanged, bonds are constantly broken and reformed in the dynamic network. DA networks in general require heat to heal macroscopic damage (Fig. 1A). Upon damage, locally the DA bonds, which are the weakest links in the network [24], are mechanically broken and the fracture surfaces are pulled apart. Healing starts by bringing the fracture surfaces back in contact. Upon reconnecting, microscopic misalignment is unavoidable and cavities are created. To fill these microscopic cavities, mobility in the network is essential, such that the material can slowly seal the openings through a “self-sealing zipping effect” (Fig. 1B). At the edges of the cavities, the exothermal formation of DA bonds and cohesive forces pull the fracture surfaces together, and the resulting self-sealing zipping effect gradually seals the entire cavity.

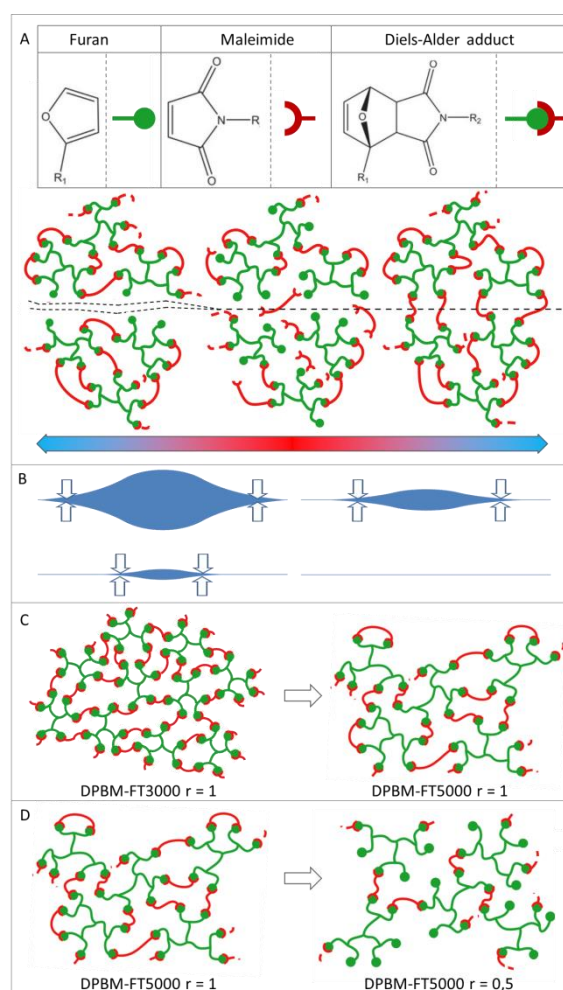


Fig. 1: A) Separated DA parts can be healed together using a mild heating treatment. The result is a strong interface due to covalent DA bonds, formed between a reactive furan and a maleimide. B) The self-sealing zipping effect in DA networks with sufficient microscopic mobility allows to slowly seal cavities. C) The molecular mobility in the network can be increased by decreasing the crosslink density, by increasing the molecular weight of the monomer units, in this case the molecular weight of the furan functionalized compound (green). D) Alternatively, crosslink density can be decreased by decreasing the maleimide-to-furan (r) ratio, by using a deficit of reactive maleimide components in the synthesis.

The mobility can be created by heating the network. Upon heating the equilibrium of the DA reaction shifts towards the unbonded state and the crosslink density will decrease, increasing the mobility (details in [9]). As a result of the

increased mobility, the cavities are slowly sealed. In this heated state, the amount of reactive components; furan and maleimides, is increased. When the cavities are completely sealed, the network is cooled down. Upon cooling, the reactive components that were formed mechanically (by the damage) and thermally (by heating), react with each other and reform the DA crosslinks. The result is that the damage is completely healed and the initial properties are entirely recovered. In other words, healing relies on two aspects: *polymer chain mobility* and *available reactive groups*.

Lowering the healing temperature

To lower the healing temperature towards room temperatures, the network mobility and the available reactive groups at 25 °C have to be increased. Network mobility can be increased through decreasing the DA crosslink density. This crosslink density is affected by the molar weight of the monomer units; a furan-functionalised compound (Fig. 1 green) and a maleimide compound (Fig. 1 red). Increasing the molar weight (e.g. from FT3000 to FT5000, details in section Reagents) decreases the crosslink density, which results in a higher molecular mobility (Fig. 1C) and a higher flexibility, expressed in lower mechanical moduli (Table 2). A second parameter that influences the crosslink density is the ratio between maleimide and furan noted r :

$$r = [M]_0/[F]_0 \quad \text{Eq. 1}$$

In which $[M]_0$ and $[F]_0$ are respectively the initial concentration of maleimide and furan used at the start of the synthesis of the network. Decreasing the r -ratio, leads to a deficit of maleimide and a decrease in crosslink density, which again increases molecular mobility (Fig. 1D and Table 2). On the other hand, a decrease in crosslink density means that upon fractures less DA bonds will be broken for a specific fracture area, which results in less “free” available reactive groups at the fracture surfaces. It is clear that the two motives for healing in DA networks, the concentration of reactive components at the fracture surfaces and the network mobility, are complementary. Higher crosslink density provides more reactive groups at the fracture surface, enhancing interfacial bonding. On the other hand, it greatly decreases the network mobility, limiting the self-sealing zipping effect. In practice, network mobility is the determining factor for healing of macroscopic damages that create relatively large cavities between the fracture surfaces.

Table 2: properties of DA polymers at 25 °C, including results of DMA (1 Hz, 0.2%) and stress-strain (1%.s⁻¹).

	r	E (MPa)	E' (MPa)	E'' (MPa)	δ
DPBM-FT3000-r1	1	139.0	202.4	23.4	6.6
DPBM-FT5000-r1	1	8.21	16.7	2.15	8.3
DPBM-FT5000-r5/6	0.833	2.40	3.98	0.58	8.2
DPBM-FT5000-r4/6	0.667	0.72	1.67	0.26	8.7
DPBM-FT5000-r3/6	0.5	0.12	0.46	0.08	9.9

For networks with higher crosslink density (DPBM-FT5000 with $r = 4/6$ or $r = 6/6$), to heal macroscopic damage, the mobility has to be increased by heating the polymer (80 - 90 °C) [12][25][14]. The decrease in DA crosslink density at these elevated temperatures does not only provide more network mobility, it also increases the number of reactive maleimide and furan groups at the fracture surface. Because of the required higher molecular network mobility, only very soft DA networks are able to heal macroscopic damages at 25 °C with high healing efficiency. In previous work, room temperature healing of DA networks was established by increasing only the number of reactive groups by judicious choice of monomers with lower molecular weight [24]. This

resulted in an increase in crosslink density and, hence, a tougher elastomer. Because of the limited molecular mobility, healing efficiencies up to 40 % could be reached at 30 °C (based on fracture stress). To increase healing efficiency, both the molecular mobility and the number of reactive components are being increased in this research paper.

In what follows, it will be experimentally demonstrated that the DPBM-FT5000 network with off-stoichiometric maleimide-to-furan ratio $r = 3/6 = r0.5$ has enough network mobility and reactive components to heal macroscopic damage at room temperature with high healing efficiency. High network mobility is translated in a highly flexible character as indicated by the mechanical properties in Table 1 and 2. Because of the low crosslink density, the available reactive components on the fracture surfaces are limited, resulting in a slow healing that takes several days to fully recover initial properties. When an increase in network mobility is required to perform healing, it is recommended to decrease the crosslink density through decreasing the maleimide-to-furan (r) ratio (like done in the $r0.5$ material) rather than to decrease both the maleimide and the furan concentration in a stoichiometric network by using larger Jeffamines. The excess of furan present in the off-stoichiometric network provides more reactive furan components on the fracture surface, which enhances healing.

Instantaneous room-temperature healing

To check the healability at room temperature, DPBM-FT5000-r0.5 samples with a width of 5.5 mm and a thickness of 2 to 2.5 mm were synthesized. A first test was performed by cutting a sample in two using a knife and immediately putting the fracture surfaces back together manually (Fig. 2A)¹. After firmly pressing the two halves together for 3 seconds, the two parts were already merged and the part could be strained a few percent without fracture. This first non-quantitative experiment illustrates that a small part of the healing is instantaneous. Upon fracture, DA bonds are broken at the surface, and reactive maleimide and furan components are generated. Upon bringing the fracture surfaces back in contact only a few seconds after damage, the available reactive components start to react with each other. The first interfacial covalent bonds as well as physical interaction, such as Van der Waals forces, and interdiffusion of pendant chains, lead to the instantaneous healing of the parts. As only few covalent bonds are formed immediately, due to slow reaction kinetics, the interface has still a very limited strength. It mainly relies on adhesion rather than on covalent bonding and the sample can only resist very limited stresses.

As for all autonomous SH networks (Table 1), this instantaneous healing works only if the fracture surfaces are brought back into contact soon after damage. If not, the available reactive groups, in this case maleimide and furan, will react with each other in the separate parts. As a result, the healing efficiency decreases significantly with too long waiting times between the damaging and re-contacting of the fracture surfaces [24]. Under the hypothesis that all bonds are broken at the fracture surfaces, the availability of the reactive maleimide and furan as function of time can be modelled using the kinetics/thermodynamics simulation (Fig. 2B). Details on the simulation can be found in [26]. In this graph the conversions are calculated using following equations:

$$x_M = \frac{[M]}{[M]_0} \wedge x_F = \frac{[F]}{[F]_0} \wedge x_{DA} = \frac{[DA]}{[M]_0} \quad \text{Eq. 2}$$

¹ Movie at <https://youtu.be/2A7eKtRixOU>

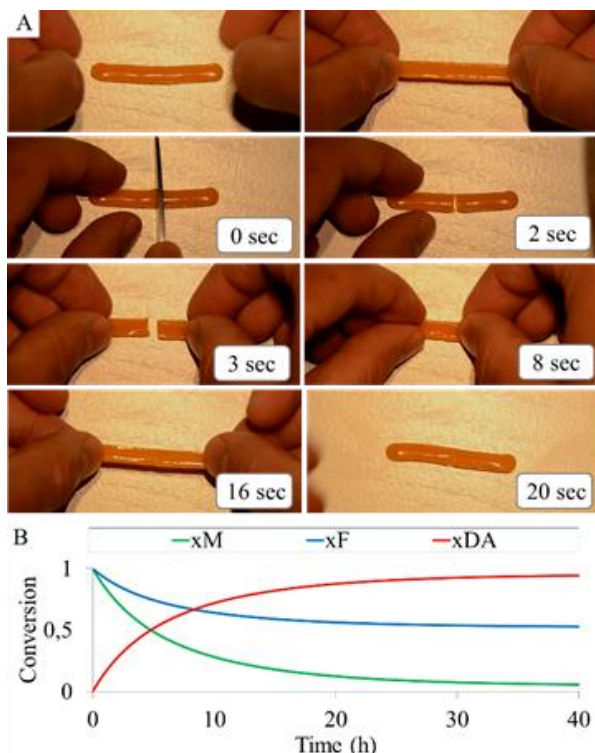


Fig. 3: A) DPBM-FT5000-r0.5 sample with a width of 5.5 mm and a thickness of 2.5 mm is cut completely in two using a knife. Immediately after cutting, the two halves are put back together manually at room temperature. After pressing the two parts together for 3 seconds, the fracture surfaces merged and the sample could already be strained a few percent without fracture.¹ B) Simulation of the relative maleimide content (x_M), the relative furan content (x_F), and the DA conversion (x_{DA}) as a function of time at 25 °C.

Looking at the maleimide content (x_M), after 1 hour only 84% of the reactive maleimide groups that were available immediately after damage are expected to be still present on the fracture surfaces. After 12 and 24 hours this is reduced to only 23% and 10%, respectively. This stresses the importance of bringing the fracture surfaces back in contact as soon as possible. Although the duration between fracture and re-mending might not influence the eventual healing efficiency, it most certainly strongly influences the speed of healing.

Healing efficiency as a function of healing time

Because of the limited amount of available reactive components at the fracture surface in low crosslink density DA networks and because of the slow reaction kinetics at 25 °C, the healing of macroscopic damages takes time. In a second experiment, the healing efficiency, based on the recovery of the fracture strain and fracture stress, is experimentally measured as a function healing time. Samples with a width of 5.5 mm and a thickness of 2 - 2.5 mm were subjected to stress-strain tensile tests until fracture (Fig. 3A). As a reference, 6 (undamaged) samples were fractured in a stress-strain test (Fig. 4A). These samples failed on average around a strain of 245% and a stress of 0.1 MPa. The Young's modulus of this material, the slope of the tangent line in the origin of the stress-strain curve, is 0.12 MPa.

Next, 24 samples were sliced in two using a clean scalpel blade (Fig. 3B). Immediately after the cut, the two ends were brought back in contact manually. When macroscopic misalignments are avoided while fitting the fracture surfaces back together, the instant healability of the DPBM-FT5000-r0.5 network allows to precisely merge the parts together, such

that the cut is no longer visible when investigated using optimal microscopy (Fig. 3 E, F and G). These samples were left to heal at room temperature for 1 day, 3 days, 7 days, or 14 days. For each healing time, 6 samples were fractured in a stress-strain test (Fig. 4A, 1 %·s⁻¹). The mean fracture stresses and strains are presented in the block diagrams in Fig. 4B. In Fig. 4C, the mean healing efficiencies for the different healing times (H_t) were calculated by comparing the fracture strains and stresses with those measured in the reference experiment:

$$\eta_{\epsilon(H_t)} = \epsilon_{fract(H_t)} / \epsilon_{fract(not\ damaged)} \quad \text{Eq. 3}$$

$$\eta_{\sigma(H_t)} = \sigma_{fract(H_t)} / \sigma_{fract(not\ damaged)} \quad \text{Eq. 4}$$

Fig. 4A illustrates that after healing at room temperature very similar stress-strain characteristics are measured, but failure occurs at much lower stresses. Creating interfacial DA bonds clearly takes time, which is due to slow reaction kinetics. After healing for 1 day at 25 °C only 50% of the fracture stress (η_{σ}) is recovered (Fig. 4C). Visual inspection showed that the fracture took place at the same location as where the cut was made previously. The formed fracture surfaces looked again clean and identical to the picture in Fig. 3B. The healing efficiencies (η_{ϵ} and η_{σ}) can be increased by prolonging the healing time. Indeed, after 3 days, 7 days, and 14 days, the fracture stress has recovered by respectively 62%, 91%, and 97%. Although the DA reactions are generally considered to be too slow for room temperature autonomous healing, the increasing failure strength over time clearly proves the contribution of the reformation of these reversible links to the healing process, at room temperature. After 14 days of healing at room temperature, the fracture did no longer take place at the location where the cut was made, but rather at a location where an imperfection causes stress concentrations (e.g., a cavity caused by a solvent bubble or a dust particle, Fig. 3D). Taking into account the standard deviations of the mean (SEM) presented on the block diagrams in Fig. 4C and the fact that fracture does not take place at the location of the “scar” of the cut, it can be concluded that after 14 days, the cuts are completely healed and that the initial strength of the samples has been recovered completely. The presented results are all obtained at 25 °C. At lower application temperatures healing takes slightly longer, while at higher temperatures, the duration of healing will be shortened.

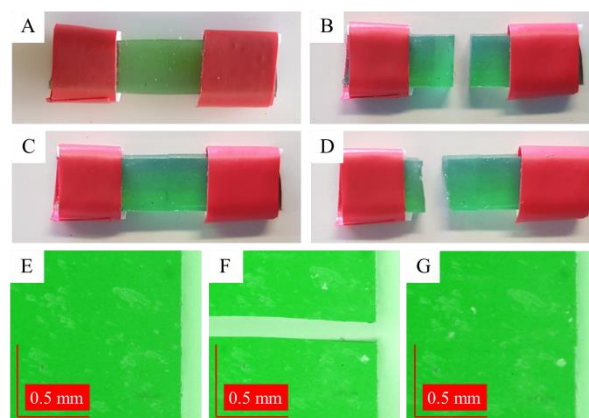


Fig. 2: Testing of autonomous healing at room temperature. A) Samples with a width of 5.5 mm, a thickness of 2-2.5 mm, and a length of 8-10 mm. B) Samples are sliced in two using a scalpel blade. C) Samples are pressed back together seconds after damage and placed at room temperature for 1 day, 3 days, 7 days, or 14 days before being subjected to a stress-strain tensile test until fracture. D) The samples that were cured for 14 days do not fracture on the location of the initial damage but on a new location. E, F, G) Microscopic images of the sample prior to damage (E), after damaged (F) and when reconnected (G).

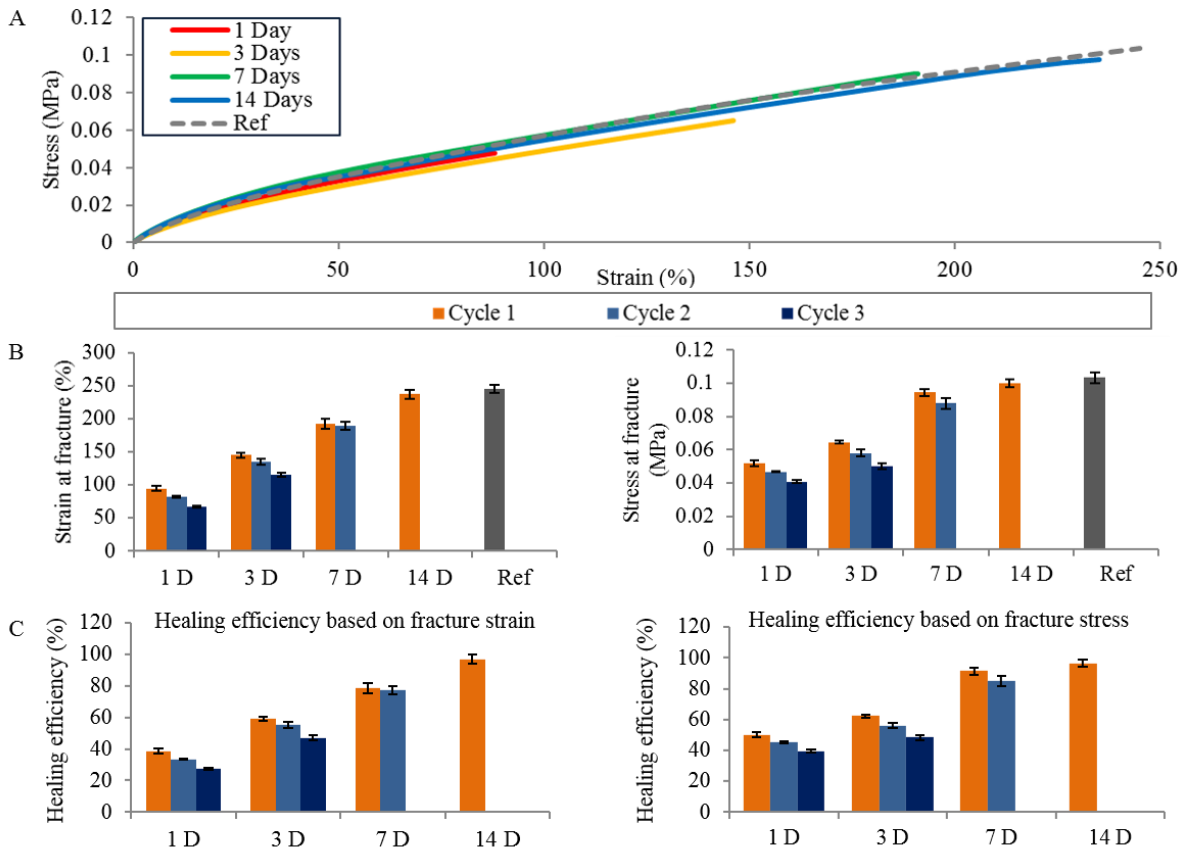


Fig. 4: A) Comparison of stress-strain curves of reference (undamaged) samples and samples that were cut all the way through and subsequently healed at room temperature for 1 day, 3 days, 7 days and 14 days. Stress-strain tests are performed with a strain ramp of $1\%s^{-1}$. B) Mean values (of 6 samples) of the strain and stress at fracture, derived through tensile testing, are presented for the reference sample and samples that are healed for 1 day, 3 days, 7 days and 14 days at $25\text{ }^{\circ}C$. C) Healing efficiencies based on the fracture strain and fractures stresses of the healed samples relative to fracture parameters of the reference samples. Error bars represent the standard error of the mean (SEM).

Healing efficiency as function of healing cycles

For the samples that were healed for 1 day, 3 days, and 7 days, immediately after fracturing the samples in the stress-strain tensile test to test the healing efficiency, the generated pieces (Fig. 3B) were brought back in contact to heal (Fig. 3C). After again healing for the same duration, 1 day, 3 days and 7 days, the samples were again fractured in the tensile tests. For all healing times, the fracture strain and fracture stress of the second healing cycle is slightly lower (Fig. 4B). A possible explanation is that at the surface of cavities, generated at the merging zone, the amount of available reactive maleimide and furan groups decreases slowly as function of time (Fig. 2B). After intermediate healing times of 1 day, 3 days, and 7 days, not all cavities are completely sealed. Consequently, when broken in the stress-strain tensile test, the resulting fracture surfaces have less reactive components on their surface compared to the fracture surfaces generated by cutting a fresh sample. As a result, the recovery of fracture strain and fracture stress will take longer in the second healing cycle.

In addition, the cavities that remained after incomplete healing can be enlarged in the first tensile test before rupture occurs. When the two parts are placed back together for the second healing cycle, the surfaces are probably matching less well, and the cavities are slightly bigger than in the first healing cycle. As a result, more extensive “zipping” is required, increasing the required duration of the healing process. For the same reasons the recovery of the initial properties in the third healing cycle is even lower than for the

second. Although not yet experimentally validated because of time limitations, the authors believe that even when fracturing a sample before all cavities are healed (e.g. after 1 day), a complete recovery of that sample can still be achieved in a next longer healing cycle (e.g. > 14 days).

Design of soft actuators that heal at room temperature

To illustrate that the DPBM-FT5000-r0.5 network is suitable to develop soft robotic components that can heal at room temperature, bending soft pneumatic actuators (BSPA), were constructed using this material. The design is based on previously published BSPAs (details on the design and working principle in [9] and [14]). The new BSPA is made entirely out of the DPBM-FT5000-r0.5. Because of the hyperelasticity of this network (Young’s modulus 0.12 MPa , derived from stress strain curve in Fig. 4A), the bottom sheet is now thicker, 3.5 mm (Fig. 5), compared to the design in [9]. If not the actuator would be too flexible, as Abaqus simulations indicated that it would deform under its own weight. By designing the bottom layer thicker, strains in this layer are limited and consequently the actuator has an anisotropic bending response to overpressure in the air chambers (Fig. 6). The manufacturing of this actuator will not be addressed in this paper as it is identical to the shaping process used for the BSPA, described in [9] and [14].

Validation of the mechanical properties

The constructed actuator was tested in a dedicated test bench containing a digital camera to measure deformations and a closed loop pressure controller to regulate the overpressure in

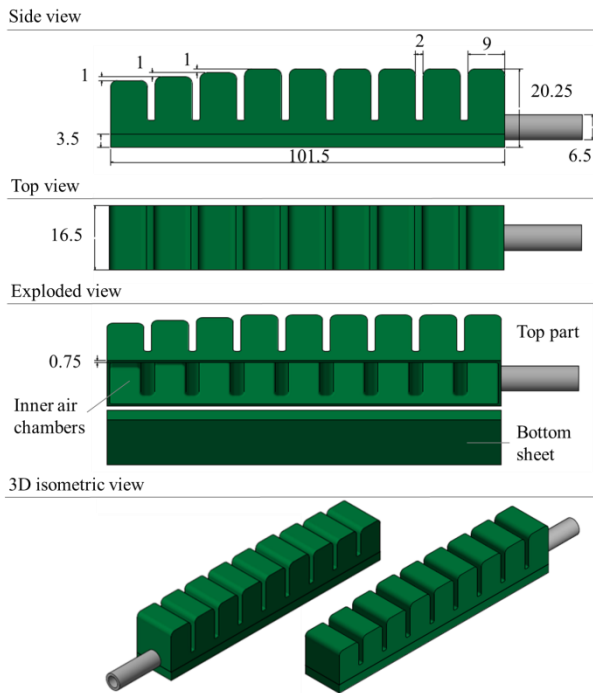


Fig. 5: Design of the self-healing bending soft pneumatic actuator completely constructed out of DPBM-FT5000-r0.5 polymer. Dimensions are presented in millimetres.

the air chambers (details of the controller in [9]). The bending characteristics, including the tip trajectory and the relation between the bending angle and the overpressure in the air-chambers for downward bending and for upward bending can be found in Fig. 6. Because of the hyperflexibility, the direction of the gravity field has an influence on this bending characteristic. This highlights the importance of adding feedback to the controller of these soft actuators. The model-free feedforward controller used in this paper is insufficient when these finger actuators are used in industrial or commercial applications, because the response characteristic of the actuators changes when orientated differently. Feedback control requires the integration of (a) sensor(s) in actuator. To not lose the desired flexible characteristic of the soft actuator,

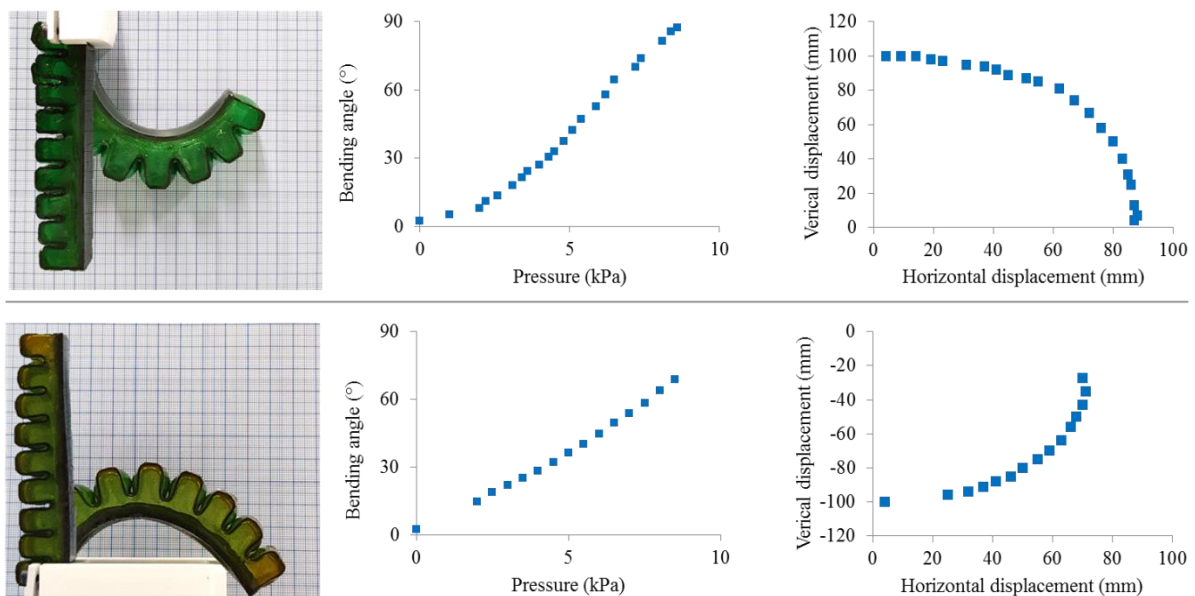


Fig. 6: The bending characteristics of the BSPA were measured using a digital camera. To check the influence of gravity the characteristic was derived for bending downwards and bending upwards. The deformation trajectory and the bending angle were measured as a function of the over-pressure of the air chambers, both when the actuators are mounted with the tip facing up and with the tip facing down.

the integrated sensor will have to be soft as well. In general, in many soft robots, feedback control is required, hence the recent development of a new field in the robotics: the “soft sensors” field. In future work soft sensors and feedback controllers will be added to the self-healing soft actuators. Five identical actuators were manufactured out of DPBM-FT5000-r0.5. By placing the five BSPAs in one soft hand assembly, their usability for social soft robotics applications was demonstrated (Fig. 7)². The five fingers can be controlled separately, which permits the hand to perform simple hand gestures that can be used in social soft robots to express emotions.

Validation of the healing ability in the soft hand

The healability of the BSPAs is demonstrated by applying macroscopic cuts all the way through the soft membranes at different locations on the actuator (Fig. 8). For these tests, a clean blade was used. The first cut (length of 12 mm and all the way through) was made in the thick bottom sheet, perpendicular to the longitudinal axis of the non-inflated actuator (Fig. 8A)³. When the blade is taken out, the elastic response of the DA material pushes the cut surfaces back together. The actuator was left untouched for only 30 seconds after which it was inflated. After only 30 seconds of healing at room temperature the actuator was airtight and could recover its activities. Airtightness was confirmed when the actuator was submerged in water and no air bubbles escaped through the membrane during actuation over the full bending range. From the previous material tests (Fig. 4A), it is known that the cut is far from fully healed after only 30 seconds. However during actuation, the freshly healed cut perpendicular to the longitudinal axis is compressed, increasing contact. As such the instantaneous adhesion that relies on secondary interactions and the very low number of covalent DA bonds are sufficient to keep the actuator airtight. The definition of full recovery of the actuator is: “when the cut is healed and remains completely airtight in the full actuation range of the actuator, while the actuator performance is recovered”. As a result, for this particular damage the actuator is fully healed after only 30 seconds. This illustrates very well the dependence of the required duration of the healing process on the size of the damage and,



Fig. 7: The five BSPAs can function together in a soft hand that illustrates the potential of autonomously healable DA materials for social soft robotic applications. The fingers can be controlled separately, which allows the hand to make simple hand gestures.²

even more, on the location of the damage. After only 30 seconds the actuator can be reused in this case. During further operation, the interfacial strength of the “scar” increases progressively because the number of interfacial DA bonds will gradually increase. Eventually all microscopic cavities at

the scar will be completely sealed and the strength at the location off the scar will be recovered.

In a second test (Fig. 8B), a cut with the same size as in the first test was made in the bottom thick sheet, but now along the longitudinal axis of the actuator. During inflation, the stresses on this cut are larger, and 30 seconds of healing time was not sufficient to make the actuator airtight again. For this cut, which has the same dimensions but another orientation, a healing time of 2 hours at room temperature is required. In the first test, after 30 seconds, we can only say there is enough adhesion to keep the cut closed, as we do not know whether DA bonds already play an important role. In the case of the cut along the longitudinal axis of the actuator stresses during actuation on the scar are higher and it is clear covalent bonds are needed to keep the actuator airtight (physical adhesion is not enough). After 2 hours, enough interfacial DA bonds were formed to keep the part airtight.

A third cut (Fig. 8C) was made in the thinner top membrane of one of the rectangular cells. In this membrane, the stresses during actuation are higher than the ones in the bottom layer. This translates in a longer healing time of 16 hours, because much more DA bonds have to be formed across the cut surfaces to ensure sufficient interfacial strength to keep the actuator airtight. However, even these damages could be healed without the need of a heat stimulus and in a relatively short time of 16 hours.

To push the healability to its limits, one of the finger actuators was completely severed (Fig. 8D). Immediately after damage, the two halves were precisely, though manually, fit together. Next, the actuator was left to heal for 7 days at room temperature. After this longer healing procedure, sufficient DA bonds should have been formed all across the large cut to re-use the actuator. To validate the recovery of the initial actuator performance, the bending characteristic of the healed actuator was measured and compared to the characteristic of the undamaged actuator (Fig. 9). The same characteristic was measured after damage, indicating that the actuator properties were fully recovered.

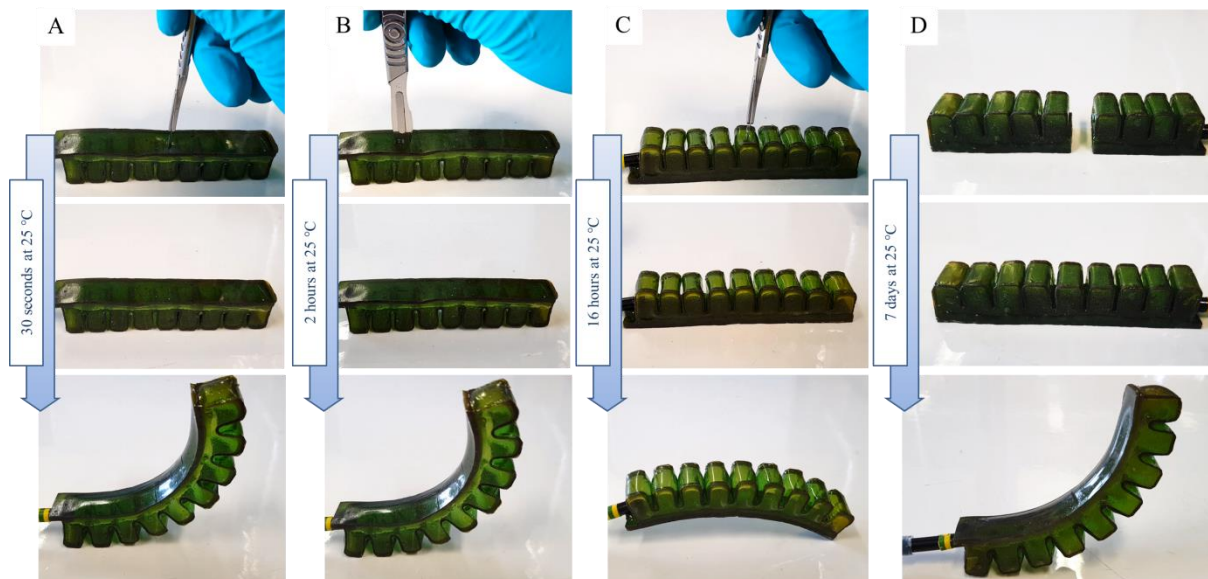


Fig. 8: The BSPAs were damaged using a scalpel blade. Macroscopic damages of different sizes and shapes were made at different locations (A-D). The duration of the healing procedure depends on the size of the damage and on the stresses that take place during actuation at the location of the “scar”. A) A 12 mm long cut all the way through the bottom layer of the actuator perpendicular to the longitudinal axis of the actuator. B) The same cut was made but along the longitudinal axis. C) A 10 mm cut, all the way through the top membrane of one of the cells of the actuator. D) The actuator was completely cut in half. All damages could be completely healed at room temperature (around 25 °C). Depending on the location of the damage the healing takes only 30 seconds or up to 7 days.³

Autonomous vs non-autonomous SH in soft robots

When using autonomous intrinsic self-healing elastomers for soft robots, there is no need for an add-on system that provides a (heat) stimulus. However, there is another advantage of these autonomous materials. When heating the DA networks, their crosslink density decreases, which affects the mechanical properties of the material. In [9][12] damages in the soft robotic components were healed by heating the entire actuator to 80 - 90 °C. When the damages were completely sealed, the parts could be cooled down to 25 °C. At 25 °C, the kinetics of the DA reaction are relatively slow and therefore it takes the material up to 24 hours to reach a near equilibrium crosslink density and recover the initial actuator properties. During autonomous healing, except for the damaged location, the crosslink density across the entire actuator remains constant. Only locally at the location of the damage, the DA concentration will change during damaging and healing. As a result, the actuator has recovered at the moment that the interfacial strength of the healed cut is high enough to withstand the local stresses that come from pressurizing the air chambers. As a result, the actuator properties will not be affected by the healing at all, providing more constant actuator properties (Fig. 9B).

A downside of using autonomous healable polymers is the loss in control over the healing process in comparison with non-autonomous healable polymers. When heat is required for the healing, the robotic system can decide when to start healing by increasing the temperature. In the case of autonomous healing, the healing will start from the moment the fracture surfaces touch. In addition, the healing should be performed right away because leaving the fracture surfaces without making contact leads to bonding of the reactive groups with each other in the separate parts. It should be noted that the lost autonomous healing potential of the aged surfaces can be replenished by a heat treatment [24]. In summary for actuators made out of non-autonomous SH DA material the healing can be performed at any desired time, while the healing in actuators made out of autonomous SH DA material should be done instantaneously after damage.

Self-contact in an actuator for very long period of time can lead to undesired merging when using autonomous SH DA materials. If for example the membranes of different cells of the actuator are in contact for several weeks or months, they will be merged as well and this can lead to a change in performance or even failure. This also applies to two different actuators which are in contact for a very long period. This merging takes longer than the healing between two freshly made fracture surfaces because not a lot of reactive maleimide and furan components are available on the surface of the actuator, in comparison with freshly formed fracture surfaces. On fracture surfaces, upon damage, a large additional portion maleimide and furan components is created by mechanically breaking of DA bonds. In the future, the formation of bonds between two surfaces with equilibrium conversion and in contact should be experimentally validated. Luckily, soft robots, like soft grippers or hands, are usually used in dynamic applications where self-contact are of short durations. If the healing time at application temperatures in next generation SH polymers in future soft robotics can be further reduced, undesired merging of planes can take place faster and definitely will have to be considered.

In this research the macroscopic damages were applied in a clean lab environment and with clean blades. Of course when evolving towards industrial and commercial applications, the

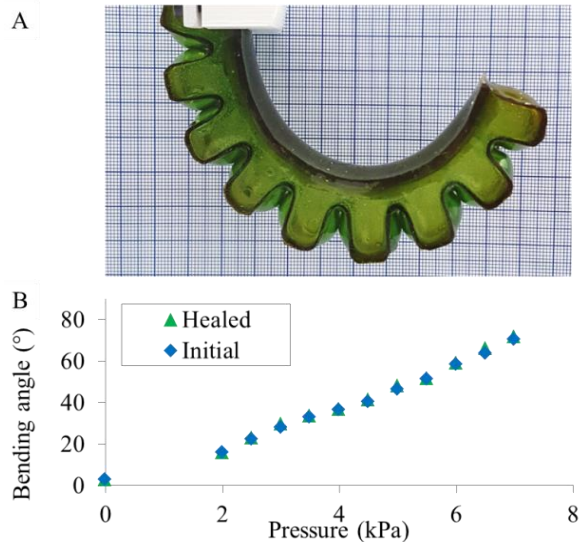


Fig. 9: A) After being cut through completely (case D from Fig. 8) and healed, the actuator was again completely airtight and could be pressurized without leaking. B) The bending characteristic of the healed actuator is compared to the initial characteristic prior to damage.

influence of contamination on the fracture surfaces on the healing performance has to be investigated. In future applications, to enhance the cleanness of the fracture surfaces, prior to healing, dirt and dust can be blown off using compressed air, available in pneumatic systems or cleaned by submerging the part in water, which can be done because the DA materials are insoluble in water.

Trade-off between mechanical properties and healing at room temperature

According to the author's knowledge, for all intrinsic SH polymer technologies (excluding healing agent-based materials), currently a general trade-off between mechanical properties (Young's modulus and tensile strength) of the SH polymer network and its healing temperature has to be considered. As a result all autonomous intrinsic SH polymers have limited mechanical strength and have a high flexibility, as illustrated in the examples in Table 1. For the DA network described in this paper the same trade-off applies. Autonomously healable DA networks have to have a lot of molecular network mobility in order to heal damage at room temperatures. Consequently, they have to be very soft. The high flexibility of these networks limit the force output of the actuators that are built from them. Soft robotic applications where higher force outputs are needed can be developed from DA material with higher Young's modulus and higher strength, such as the DPBM-FT5000-r1 material [12][14]. However, these networks have less molecular mobility. The temperature has to be increased substantially (near 90 °C) before sufficient molecular mobility allows to close and heal relevant macroscopic damages. Currently, a DA network with high mechanical properties and a healing mechanism that performs at room temperature cannot be synthesized.

Conclusion

For the first time soft robotic actuators were developed that are able to recover their performance after severe damage at room temperature, without the need for an externally applied stimulus. These were constructed from a newly developed autonomous self-healing polymer network, excluding the need of additional heating devices that would increase the complexity of the overall robotic system. The SH polymer network that is based on the reversible Diels-Alder (DA)

reaction, was designed to increase the molecular mobility by means of working at a low maleimide-to-furan ratio. This lowers the crosslink density and results in an excess of furan groups, compensating the lower maleimide concentration. A DA network was synthesised that can heal catastrophic macroscopic damage autonomously at room temperature. The healing efficiency of a fractured part, evaluated through the recovery of the stress at fracture, is 62%, 91%, and 97%, after 3 days, 7 days, and 14 days, respectively.

This material was used to develop a healable soft pneumatic hand. Relevant large cuts could be healed entirely, without the need of a heat stimulus. Depending on the size of the damage and, even more, on the location of the damage, the healing takes only seconds or up to a week. For this evaluation, the actuator was considered to be healed whenever it is completely airtight and the scar does not tear open during actuation. Damage on locations on the actuator that are subjected to very small stresses during actuation was healed instantaneously. Although only a limited amount of DA bonds is formed across the merged fracture surfaces in seconds, this provides sufficient interfacial strength to keep the actuator airtight during actuation. Severe damage, like cutting the actuator in two, took 7 days to heal, without the need of any external heat stimulus and resulted in full recovery of the actuator performance.

Reagents

Furfuryl glycidyl ether (FGE, 96 %) and 1,1'-(methylenedi-1,4-phenylene)bismaleimide (DPBM, 95%) were obtained from Aurora Chemicals. Jeffamine JT5000 and JT3000 (poly(propylene glycol) bis(2-aminopropyl ether) with average molecular weight of 5649 g.mol⁻¹ and 2916 g.mol⁻¹ (NMR) were obtained from Aurora Chemicals.

References

[1] M. T. Tolley *et al.*, “A resilient, untethered soft robot,” *Soft Robotics*, vol. 1, no. 3, pp. 213–223, 2014.

[2] R. V. Martinez, A. C. Glavan, C. Keplinger, A. I. Oyetibo, and G. M. Whitesides, “Soft actuators and robots that are resistant to mechanical damage,” *Advanced Functional Materials*, vol. 24, no. 20, pp. 3003–3010, 2014.

[3] J. Hughes, U. Culha, F. Giardina, F. Guenther, A. Rosendo, and F. Iida, “Soft Manipulators and Grippers: A Review,” *Frontiers in Robotics and AI*, vol. 3, p. 69, 2016.

[4] J. Shintake, V. Cacucciolo, D. Floreano, and H. Shea, “Soft Robotic Grippers,” *Advanced Materials*, vol. 30, no. 29, p. 1707035, 2018.

[5] A. D. Marchese, R. K. Katzschmann, and D. Rus, “A recipe for soft fluidic elastomer robots,” *Soft Robotics*, vol. 2, no. 1, pp. 7–25, 2015.

[6] D. Rus and M. T. Tolley, “Design, fabrication and control of soft robots,” *Nature*, vol. 521, no. 7553, pp. 467–475, 2015.

[7] C. Laschi, B. Mazzolai, and M. Cianchetti, “Soft robotics: Technologies and systems pushing the boundaries of robot abilities,” *Science Robotics*, vol. 1, no. 1, p. eaah3690, 2016.

[8] R. Pfeifer, H. G. Marques, and F. Iida, “Soft robotics: The next generation of intelligent machines,” *IJCAI International Joint Conference on Artificial Intelligence*, pp. 5–11, 2013.

[9] S. Terryn, J. Brancart, D. Lefeber, G. Van Assche, and B. Vanderborght, “Self-healing soft pneumatic robots,” *Science Robotics*, vol. 2, no. 9, 2017.

[10] S. Terryn, G. Mathijssen, J. Brancart, D. Lefeber, G. Van Assche, and B. Vanderborght, “Development of a self-healing soft pneumatic actuator: a first concept,”

Bioinspiration & Biomimetics, vol. 10, no. 4, p. 046007, 2015.

[11] S. Terryn, J. Brancart, D. Lefeber, G. Van Assche, and B. Vanderborght, “A pneumatic artificial muscle manufactured out of self-healing polymers that can repair macroscopic damages,” *IEEE Robotics and Automation Letters*, vol. 3, no. 1, pp. 16–21, 2017.

[12] E. Roels, S. Terryn, J. Brancart, G. Van Assche, and B. Vanderborght, “A multi-material self-healing soft gripper,” in *IEEE International Conference on Soft Robotics (RoboSoft)*, 2019, pp. 316–321.

[13] J. Brancart, G. Scheltjens, T. Muselle, B. Van Mele, H. Terryn, and G. Van Assche, “Atomic force microscopy based study of self-healing coatings based on reversible polymer network systems,” *Journal of Intelligent Material Systems and Structures*, vol. 25, no. 1, pp. 40–46, 2014.

[14] S. Terryn, E. Roels, G. Van Assche, and B. Vanderborght, “Self-Healing and High Interfacial Strength in Multi-Material Soft Pneumatic Robots via Reversible Diels-Alder Bonds,” *Actuators: Special issue on pneumatic soft actuators*, vol. 9, no. 34, pp. 1–17, 2020.

[15] B. Willocq, R. K. Bose, F. Khelifa, S. J. Garcia, P. Dubous, and J. M. Raques, “Healing by Joule effect of electrically-conductive poly(esterurethane) carbon nanotubes nanocomposites,” *Journal of Materials Chemistry B*, vol. 4, no. 11, pp. 4089–4097, 2016.

[16] S. R. White *et al.*, “Autonomic healing of polymer composites,” *Nature*, vol. 409, no. 6822, pp. 794–797, 2001.

[17] L. Leibler, P. Cordier, and C. Soulie, “Self-healing and thermoreversible rubber from supramolecular assembly,” *Nature*, vol. 451, no. 7181, pp. 977–980, 2008.

[18] G. M. L. Van Gemert, J. W. Peeters, S. H. M. Söntjens, H. M. Janssen, and A. W. Bosman, “Self-healing supramolecular polymers in action,” *Macromolecular Chemistry and Physics*, vol. 213, no. 2, pp. 234–242, 2012.

[19] “www.suprapolix.com.”

[20] R. Adam Bilodeau and R. K. Kramer, “Self-healing and damage resilience for soft robotics: A review,” *Frontiers Robotics AI*, vol. 4, no. OCT, 2017.

[21] Y. Chen, A. M. Kushner, G. A. Williams, and Z. Guan, “Multiphase design of autonomic self-healing thermoplastic elastomers,” *Nature Chemistry*, vol. 4, no. 6, p. 467, 2012.

[22] C. Li *et al.*, “A highly stretchable autonomous self-healing elastomer,” *Nature Chemistry*, vol. 8, no. 6, pp. 618–624, 2016.

[23] A. Rekondo, R. Martin, and A. R. De Luzuriaga, “Catalyst-free room-temperature self-healing elastomers based on aromatic disulfide metathesis,” *Materials Horizon*, vol. 20, pp. 3–6, 2013.

[24] M. M. Diaz, J. Brancart, G. Van Assche, and B. Van Mele, “Room-temperature versus heating-mediated healing of a Diels-Alder crosslinked polymer network,” *Polymer*, vol. 153, pp. 453–463, 2018.

[25] E. Roels, S. Terryn, J. Brancart, R. Verhelle, G. Van Assche, and B. Vanderborght, “Additive Manufacturing for Self-Healing Soft Robots,” *Soft Robotics*, vol. 00, no. 00, pp. 1–13, 2020.

[26] A. Cuvellier, R. Verhelle, J. Brancart, B. Vanderborght, G. Van Assche, and H. Rahier, “Polymer Chemistry The influence of stereochemistry on the reactivity of the Diels-Alder cycloaddition,” *Polymer Chemistry*, vol. 10, no. 4, pp. 473–485, 2019.

Funding: Funded by the FWO (Fonds Wetenschappelijk Onderzoek): personal FWO-grants of Terryn (FWOTM784), Brancart (12W4719N) and Roels (1S84120N) and by the EU FET SHERO (828818).